Published in final edited form as:
Neuroimage. 2012 January 16; 59(2): 1190–1199. doi:10.1016/j.neuroimage.2011.08.009.

Anticorrelated Resting-state Functional Connectivity in Awake Rat Brain

Zhifeng Liang[*], **Jean King**[*], and **Nanyin Zhang**[*,¶]

[*]Center for Comparative Neuroimaging, Department of Psychiatry, University of Massachusetts Medical School, Worcester, Massachusetts 01655

Abstract

Resting-state functional connectivity (RSFC) measured by functional magnetic resonance imaging has played an essential role in understanding neural circuitry and brain diseases. The vast majority of RSFC studies have been focused on positive RSFC, whereas our understanding about its conceptual counterpart—negative RSFC (i.e. anticorrelation)—remains elusive. To date, anticorrelated RSFC has yet been observed without the commonly used preprocessing step of global signal correction. However, this step can induce *artifactual* anticorrelation (Murphy et al., 2009), making it difficult to determine whether the observed anticorrelation in humans is a processing artifact (Fox et al., 2005). In this report we demonstrated robust anticorrelated RSFC in a well characterized frontolimbic circuit between the infralimbic cortex (IL) and amygdala in the awake rat. This anticorrelation was anatomically specific, highly reproducible and independent of preprocessing methods. Interestingly, this anticorrelated relationship was absent in anesthetized rats even with global signal regression, further supporting its functional significance. Establishing negative RSFC independent of data preprocessing methods will significantly enhance the applicability of RSFC in better understanding neural circuitries and brain networks. In addition, combining the neurobiological data of the IL-amygdala circuit in rodents, the finding of the present study will enable further investigation of the neurobiological basis underlying anticorrelation.

Keywords

resting state; functional connectivity; anticorrelation; rat; amygdala; infralimbic cortex

Introduction

Resting-state functional connectivity (RSFC) has been intensively and extensively studied using functional magnetic resonance imaging (fMRI) (Biswal et al., 1995). Resting-state fMRI (rsfMRI) measures spatial patterns of functional connectivity across the brain by detecting temporal correlations of low-frequency spontaneous fluctuations of the blood-oxygenation-level dependent (BOLD) signal. Using this technique, RSFC was consistently revealed in multiple networks in humans (Biswal et al., 1995; Greicius et al., 2003;

[¶]Correspondence Authors: Nanyin Zhang, Ph.D Nanyin Zhang, Ph.D. Assistant Professor Center for Comparative Neuroimaging (CCNI) Department of Psychiatry University of Massachusetts Medical School 55 Lake Avenue North Worcester MA 01655 Tel: 508-856-5482 Fax: 508-856-8090 Nanyin.Zhang@umassmed.edu.

Hampson et al., 2002; Lowe et al., 1998) and animals (Liang et al., 2011; Vincent et al., 2007; Zhang et al., 2010), and was sensitive to effects like sleep, anesthesia and aging (Horovitz et al., 2009; Stevens et al., 2008). Additionally, altered RSFC was found in multiple pathological conditions (Greicius et al., 2007), indicating its vital neurobiological and psychopathological relevance (Albert et al., 2009; Kennedy et al., 2006). Taken together, it has been strongly suggested that RSFC plays a very important role in brain function.

Conceptually, temporal correlations of spontaneous BOLD fluctuations between functionally connected brain regions should include both positive and negative values. More importantly, positive and negative correlations in RSFC are most likely related to distinct neurophysiologic substrates underlying functional connections. To date, predominant efforts have been spent investigating positive RSFC, whereas negative correlation (i.e. anticorrelation) has been much less studied.

Anticorrelation was first reported between the default mode network (DMN) and task-positive network (TPN) in the human (Fox et al., 2005). This temporally inverse correlation in spontaneous BOLD fluctuations was initially interpreted as competition or functional segregation for opposite goals between neural networks. Further, the strength of this anticorrelation was associated with response time in cognitive functions (Kelly et al., 2008) and performance in working memory tasks (Hampson et al., 2010). However, these interpretations were complicated by one commonly used fMRI preprocessing procedure-global signal regression (Murphy et al., 2009). This procedure was used to remove global physiological noise in resting-state functional images, and thus improved the spatial specificity of RSFC (Fox et al., 2009; Scholvinck et al., 2010). However, Murphy *et. al*. in their recent study pointed out that global signal removal can induce artifactual anticorrelation. This is because removal of the global signal ensures that the sum of correlation coefficients across all voxels within the whole brain must approach zero, and thus this procedure mandated anticorrelation (Murphy et al., 2009). Although several preprocessing methods were proposed subsequently in hope to overcome the limitation of global signal regression, contradicting results were obtained (Anderson et al., 2010; Chang and Glover, 2009). For instance, it was reported that anticorrelation between DMN and TPN was present with or without model-based physiological noise correction (Chang and Glover, 2009) and this anticorrelation was not static (Chang and Glover, 2010). Anderson and colleagues, however, reported the absence of anticorrelation between DMN and TPN using phase-shifted soft tissue regression (Anderson et al., 2010).

The ambiguity of anticorrelated RSFC has become a major obstacle to further understanding its neurophysiologic mechanism and has significantly limited its applicability. Therefore, validating the existence of anticorrelation that is independent of preprocessing methods is of critical importance particularly considering the possibility that negative RSFC might represent a group of functional connections with a distinct neurophysiologic mechanism and thus could be crucial for better understanding of neural circuitries and brain diseases. In order to achieve this goal, identifying a neural circuit with robust negative RSFC is a crucial step.

Well-documented reports of the neural circuit between infralimbic cortex (IL) and amygdala in the rat (Pape and Pare, 2010) have shed light on the aforementioned issue. This frontolimbic circuit has been extensively studied in several aspects: Anatomically, IL and amygdala share dense reciprocal interconnections (McDonald, 1998; Russchen, 1982a, 1982b; Sesack et al., 1989). Functionally, neurobiological evidence indicates that IL plays a role of inhibitory regulation of the amygdala (Rosenkranz and Grace, 2001). Specifically, IL sends glutamatergic projections to intercalated cells of the amygdala (Amano et al., 2010;

Berretta et al., 2005). Intercalated interneurons in turn send GABAergic projections to central amygdala nucleus, thus enabling IL to exert inhibitory modulation on amygdala. Additionally, electrophysiological studies indicate that the stimulation of IL area suppresses the basolateral amygdala activity (Likhtik et al., 2005; Rosenkranz and Grace, 2001), and decreases the responsiveness of central amygdala (Quirk and Gehlert, 2003; Quirk et al., 2003). Based on these findings, we hypothesize that anticorrelated RSFC should be present within the IL-amygdala circuit. To test this hypothesis, in the current study we have systematically examined the temporal relationship of spontaneous BOLD fluctuations between IL and amygdala using rsfMRI in awake and isoflurane-anesthetized rats (Liang et al., 2011; Zhang et al., 2010). We reported robust anticorrelated RSFC within the IL-amygdala circuit regardless of global signal regression in awake rats. This anticorrelation, however, disappeared in anesthetized rats even with global signal regression. Time-frequency dynamics of this negative functional connectivity were also examined using wavelet analysis.

Methods

Animals

Twenty four adult male Long-Evans (LE) rats (300 – 400 g) were obtained from Charles River Laboratories. Animals were housed in Plexiglas cages and maintained in ambient temperature (22–24 °C) on a reversed 12-h light:12-h dark cycle. Food and water were provided *ad libitum*. All studies were approved by IACUC Committee of the University of Massachusetts Medical School.

Acclimation procedure

Rats were acclimated to MRI restraint and noise as described in our previous studies (King et al., 2005). Briefly, rats were anesthetized with isoflurane and secured in Plexiglas stereotaxic head holders using plastic ear-bars. EMLA cream was applied topically to minimize pain of mechanical restraint. Animals were then placed into a black opaque tube 'mock scanner' with tape-recorded scanner noises. Animals were acclimated for eight days, one session per day. The time of exposure was increased from 15 minutes on the first day to 90 minutes on days 6, 7 and 8, with an increment of 15 minutes per day.

Animal preparation

Animal was briefly anesthetized using isoflurane and fitted into a head restrainer with a built-in coil. The head was placed into the cylindrical head-holder with the canines secured over a bite bar, the nose secured with a nose clamp, and ear bars positioned inside the head-holder with adjustable screws fitted into lateral sleeves. The body of the animal was then placed into a body restrainer. After this setup procedure was completed, the isoflurane was removed and the restraining system was positioned in the magnet for imaging under awake condition.

Rats (16 of the 24) underwent the imaging session in the anesthetized condition at minimal 7 days after being imaged at the awake condition. The animal preparation procedure was the same as in the awake condition. Isoflurane gas (2%) was then delivered to the animal through a nose cone in the magnet to maintain the anesthetized state. The body temperature of the animal was monitored and maintained at 37°C ± 0.5°C using a feedback controlled heating pad. Imaging sessions started at least 15–20 mins after animals were placed in the magnet.

MR experiments

All experiments were carried out on a Bruker 4.7T/40cm horizontal magnet (Oxford, UK) interfaced with a Biospec Bruker console. A dual ^{1}H radiofrequency (RF) coil configuration (Insight NeuroImaging Systems, Worcester, MA) consisting of a volume coil for exciting the water proton spins and a surface coil for receiving MRI signal was used. The volume and surface coils were actively tuned and detuned to prevent mutual coil coupling.

For each session, anatomical images were acquired using a fast spin-echo sequence (RARE) with the following parameters: TR = 2125ms, RARE factor = 8, TE = 50ms, matrix size = 256×256, FOV = 3.2cm×3.2cm, slice number = 18, slice thickness = 1mm. Gradient-echo images covering the whole brain were then acquired using the echo-planar imaging (EPI) sequence with the following parameters: TR = 1s, TE = 30ms, flip angle = 60°, matrix size = 64×64, FOV = 3.2cm×3.2cm, slice number=18, slice thickness = 1mm. Two hundred volumes were acquired for each run, and six runs were obtained for each session.

Pre-processing of imaging data

Part of the raw rsfMRI data (16 out of 24 rats) were from a previous study (Liang et al., 2011) and reprocessed for the purpose of the present study. Data from the other 8 (out of 24) rats were acquired for the present study.

Imaging data was preprocessed using Medical Image Visualization and Analysis (MIVA, http://ccni.wpi.edu/), Statistical Parametric Mapping (SPM8) software (Wellcome Department of Cognitive Neurology, London, UK) and MATLAB (Mathworks, Inc., Sherborn, MA). All images were first aligned and co-registered to a fully segmented standard rat atlas in MIVA (Liang et al., 2011; Zhang et al., 2010). The registration procedure provided the coordinates of each seed ROI in the image space. In this study two seed regions of interest, bilateral IL and bilateral amygdala, as well as a control seed region, unilateral (right) motor cortex, were selected (as shown in Figure 1). After registration, all functional images were pre-processed with steps of motion correction, spatial smoothing (FWHM = 1mm), voxel-wise linear detrending and 0.002#x2013;0.1Hz bandpass filtering. Data sets with excessive motion (>0.5 mm, 17 runs in total) were discarded. The time course for each individual voxel was further corrected for head movement by regression on the six motion parameters (translations and rotations) estimated in the procedure of motion correction. The global signal was estimated by averaging the time courses of all voxels inside the whole-brain mask. The ventricle and white matter signal was estimated by averaging the time courses of all voxels inside the ventricle and white matter.

Functional connectivity analysis

Functional connectivity was evaluated using seed-based correlational analysis on a voxel-by-voxel basis (Zhang et al., 2010). Regionally averaged time courses from all voxels inside the seed regions were used as reference time courses. Pearson cross-correlation coefficients between reference time courses and the time course of each individual voxel were calculated. This correlational analysis was carried out for each run. Correlation coefficients were transformed using Fisher's z transformation and then averaged across runs and animals. Subsequently, the averaged z values were transformed back to r values, yielding a mean correlation map for each seed. RSFC maps were displayed by thresholding the correlation coefficient at 0.21 and a cluster size of 10 voxels (equivalent to uncorrected $p<0.001$) (Forman et al., 1995).

The reliability of functional connectivity was examined through inter-subject reproducibility. Animals were randomly divided into two subgroups and functional connectivity maps were separately created for each group. The strength of functional

connectivity was quantitatively compared on the voxel-by-voxel basis between the two subgroups.

Wavelet analysis

Wavelet transform coherence (WTC) was previously utilized for analyzing dynamic changes between rsfMRI time series (Chang and Glover, 2010). This approach was used in the present study to investigate the dynamics of the anticorrelated relationship between time courses of IL and amygdala. Briefly, the continuous wavelet transform of a time series (x_n, n=1,2…N) with equal time step Δt was defined as:

$$W^X(n,s) = \sqrt{\frac{\Delta t}{s}} \sum_{n'=1}^{N} \chi_n \psi^0 \left[(n'-n) \left(\frac{\Delta t}{s} \right) \right] \quad [1]$$

where n is the time index, s is the time scale, and ψ^0 is the Morlet wavelet as follows:

$$\psi_0(\eta) = \pi^{-1/4} e^{i\omega_0 \eta} e^{-\frac{1}{2}\eta^2} \quad [2]$$

where ω_0 is dimensionless time and set at 6, η is dimensionless frequency. The wavelet power was defined as $|W^X(n,s)|^2$. Similarly, the cross wavelet transform (XWT) for two time series is defined as

$$W^{XY}(n,s) = W^X(n,s)\, W^{Y*}(n,s) \quad [3]$$

Where * denotes complex conjugation. XWT evaluates the common power of two time series in time frequency space. To evaluate the coherence of cross wavelet transform, cross wavelet coherence was calculated as follows:

$$R_n^2(s) = \frac{\left| S\left(s^{-1} W_n^{XY}(s) \right) \right|^2}{S\left(s^{-1} |W_n^X(s)|^2 \right) \cdot S\left(s^{-1} |W_n^Y(s)|^2 \right)} \quad [4]$$

Cross wavelet coherence can be seen as local “correlation coefficients” in time frequency space. The statistical significance was determined using Monte Carlo methods. Wavelet transform coherence and cross-wavelet transform were implemented with a matlab toolbox provided by Grinsted et. al. (http://www.pol.ac.uk/home/research/waveletcoherence/), and detailed information could be found in Ref. (Grinsted et al., 2004).

Results

Anticorrelated relationship between amygdala and infralimbic cortex

Figure 2 showed the RSFC maps from the seed of IL. Anticorrelated functional connectivity between IL and amygdala was evident without any global signal correction (referred to as “uncorrected” hereafter) (Fig 2a). Interestingly, negative RSFC from IL was only observed in amygdala while positive RSFC was widely spread across cortical and subcortical areas. With the correction of the global signal (Fig 2c), the spatial location of anticorrelation remained in amygdala. In addition, anticorrelation was also observed in some other regions such as hypothalamus (HT) after global signal regression. By contrast, the wide spread positive RSFC seen in the uncorrected map was greatly confined to more anatomically

specific regions including anterior cingulate cortex (ACC), septum, caudate-putamen (CPU), neuclus accumbens (NAcc), and dorsal lateral prefrontal cortex (dlPFC). These results were consistent with the previous literature suggesting that global signal regression significantly improved the spatial specificity of positive RSFC (Fox et al., 2009). The RSFC map obtained after removing the white matter and ventricle signal (Fig. 2b) showed an intermediate pattern between the uncorrected map (Fig. 2a) and the map corrected for the global signal (Fig. 2c), also consistent with the results in human studies (Fox et al., 2009).

The reciprocal anticorrelated relationship between the amygdala and IL can be observed in the RSFC maps from the amygdala as shown in Figure 3. Negative RSFC was clearly observed in IL in the uncorrected map (Fig. 3a). Similarly, corrections of the ventricle and white matter signal (Fig. 3b) as well as the global signal (Fig. 3c) significantly improved the spatial specificity of positive RSFC between amygdala and HT, as well as between amygdala and hippocampus. The anticorrelation between amygdala and IL remained largely the same. Additionally, some other regions such like CPU also showed an anticorrelated relationship with amygdala after global signal removal. Figure 2 and 3 collectively showed high anatomical specificity of the reciprocal anticorrelated relationship between the amygdala and IL.

Absence of anticorrelation in anesthetized rats

Considering that one major function of the IL-amygdala circuitry is regulating affective behaviors, it can be expected that anesthesia will disrupt the functional connectivity within the IL-amygdala circuit. Indeed, our data showed that the anticorrelated relationship between IL and amygdala observed in awake rats was completely abolished in isoflurane-anesthetized rats even with the global signal correction as shown in both Fig 2d and Fig 3d. This remarkable difference indicated that: i) the anticorrelated relationship observed in awake rats was not induced by preprocessing methods because the same preprocessing methods were applied to both awake and anesthetized rats data, and ii) the anticorrelation between amygdala and IL has important functional relevance that is impacted by anesthesia.

RSFC maps of unilateral motor cortex

In order to examine the specificity of the anticorrelation between amygdala and IL, a control seed region unilateral motor cortex was also selected. Figure 4 demonstrated the RSFC maps of unilateral (right) motor cortex in awake (Fig. 4a) and anesthetized (Fig. 4b) rats, respectively. Both maps were obtained after the global signal regression. In awake rats, we observed strong functional connections between right and the left motor cortices, whereas this bilateral connection was less apparent in anesthetized rats. This result is consistent with the notion that anesthesia reduced the strength of RSFC (Liu et al., 2010). More importantly, no anticorrelated RSFC was observed in either awake or anesthetized group, suggesting that the anticorrelated relationship observed between IL and amygdala was specific to the frontolimbic circuit as oppose to a general effect.

Distributions of correlation coefficients of RSFC between IL and amygdala

It was previously reported that global signal regression dramatically changed the distribution of computed correlation coefficients in RSFC maps: (i) artifactual negative correlations were induced, and (ii) the distribution became approximately normal with a mean correlation value close to zero (Fox et al., 2009). In the present study, we independently extracted regional mean time courses from amygdala and IL for each run, with or without global signal regression, and calculated their temporal correlation coefficients. Figure 5 showed the histograms of correlation coefficients before (Fig. 5a) and after (Fig. 5b) global signal regression. The distribution of correlation coefficients indeed shifted towards a Gaussian shape with global signal regression (Fig 5b). Nevertheless, the majority of correlation

coefficients was in the negative range regardless of global signal regression (Fig. 5a, mean correlation coefficient = −0.20, Fig. 5b, mean correlation coefficient = −0.37).

Reliability of anticorrelation between amygdala and infralimbic cortex

To test the reliability of the anticorrelated relationship between spontaneous BOLD fluctuations in amygdala and IL, data from all animals were randomly divided into two subgroups and a RSFC map, with the seed of IL, was individually obtained for each subgroup. Figure 6a and 6b showed the RSFC maps from the two subgroups, demonstrating excellent consistency. Quantitatively, the computed correlation coefficients between the two RSFC maps well agree with each other on a voxel-byvoxel basis (Fig. 6c, $r = 0.58$, $p < 10^{-5}$). Similar results can be obtained from the seed of amygdala (data not shown). These results suggest that the anticorrelated relationship between amygdala and IL observed in awake rats was highly reliable.

Time-frequency dynamics of anticorrelation between amygdala and infralimbic cortex

WTC was utilized to investigate time-frequency dynamics of the anticorrelated relationship between amygdala and IL, with and without global signal regression. We observed a strong anti-phase relationship in cross-wavelet power and wavelet transform coherence between the time courses of IL and amygdala (Figure 7 showed one example), and this anti-phase relationship was relatively consistent throughout the whole scan. In addition, the anti-phase relationship was evident without global signal regression.

Discussion

In the present study we have characterized the anticorrelated temporal relationship between spontaneous BOLD fluctuations in IL and amygdala in awake rats. To the best of our knowledge, this is the first study investigating negative RSFC in animals. Independent of preprocessing methods, we observed robust anticorrelation within this anatomically well-defined frontolimbic circuit. In addition, this anticorrelation was highly reliable as reflected from its high reproducibility between two randomly divided subgroups. Moreover, this anticorrelation was between two distinct and distant anatomical regions, and contained high anatomical specificity. Furthermore, the anticorrelated relationship between the two regions was absent in anesthetized rats even with global signal regression. Taken together, data of the present study have provided strong evidence validating the existence of anticorrelated RSFC.

The influence of global signal regression

Although the presence of anticorrelation was independent of global signal regression, it was noticeable that global signal regression indeed affected the spatial pattern of RSFC maps and the distribution of correlation coefficients. Consistent with previous reports (Fox et al., 2009), global signal removal significantly improved the spatial specificity of positive RSFC. Interestingly, global signal regression enlarged areas of negative RSFC. Compared to uncorrected maps, additional regions such as hypothalamus (HT) showed anticorrelated relationship with IL (Fig.2c), and CPU showed anticorrelated relationship with amygdala (Fig. 3c). Although the origin of these enlarged anticorrelated areas after global signal removal was not clear, we speculate that it could result from the propagation effect of indirect connectivity. It is well known that amygdala and HT are tightly connected as part of the amygdala-hypothalamic-pituitary-adrenal axis which is responsible for the autonomic stress/fear body response. This functional connection resulted in positive correlations between BOLD fluctuations in amygdala and HT as shown in Figs. 3b and 3c. Since IL and amygdala contained an anticorrelated relationship in their BOLD fluctuations, it can be predicted that this anticorrelated relationship would propagate to areas that were positively

correlated to amygdala such as HT. This propagation effect, being masked by the global signal in uncorrected maps, became detectable after the global signal was removed. Similar argument can be used to explain the anticorrelation between amygdala and CPU appeared after global signal regression. However, it has to be noted that we cannot rule out the possibility that IL and HT are directly connected with an anticorrelated relationship. Further experiments are needed to resolve this issue.

The distribution of correlation coefficients between IL and amygdala was also altered by global signal regression, shifting to an approximately normal distribution centered at about CC=−0.37. However, it did not change the sign of the majority of correlation values. Taken together, although global signal regression indeed affected the resultant RSFC maps as expected (Murphy et al., 2009), it was clearly not attributing to the anticorrelated RSFC observed between IL and amygdala.

Impact of Anesthesia

The anticorrelated relationship between IL and amygdala was absent in the anesthetized condition. Accumulating evidence has suggested that anesthesia profoundly affects RSFC. For instance, Lu and colleagues demonstrated a dose-dependent decrease of cross-hemispheric functional connectivity in α-chloralose-anesthetized rats (Lu et al., 2007). Similarly, Liu et. al. found that intrinsic BOLD fluctuations and functional connectivity in the resting rat were strongly dependent on anesthesia depth (Liu et al., 2010). In human subjects, functional connectivity in the motor cortices was completely ablated with deep anesthesia (Peltier et al., 2005). Taken together, these results suggest that anesthesia significantly weakens RSFC relative to the awake condition. In the present study, anesthesia weakened the positive RSFC between left and right motor cortex (Fig. 4), and completely abolished the negative RSFC between IL and amygdala regardless of preprocessing procedures (Fig. 2d and Fig. 3d). These results were in line with previous animal imaging studies indicating that anesthesia reduces the amplitude of RSFC (Liu et al., 2010). More importantly, distinct difference between awake and anesthetized rats further ruled out the possibility that the anticorrelation observed at the awake condition was a processing artifact because the same preprocessing procedures were applied to both conditions. Furthermore, our data demonstrated that RSFC might serve as a sensitive marker for the functionality of brain circuitry given the fact that the IL-amygdala circuit is critically involved in affective behaviors that are impacted by anesthesia. This result also provided important evidence supporting the advantage of measuring RSFC in awake animals particularly in studies of neural circuitries subserving cognitive and emotional functions (Liang et al., 2011; Zhang et al., 2010).

Possible Neural Mechanism

The anatomy and function of the IL-amygdala circuit have been well studied using various methods. These studies may shed light on understanding the neural mechanism underlying the negative RSFC within this circuit. It is well known that the IL-amygdala circuitry is implicated in affective behaviors such as fear conditioning and extinction in rodents (LeDoux, 2000), as well as in emotion regulation in humans and nonhuman primates (Phelps et al., 2004; Phelps and LeDoux, 2005). In addition, malfunction in this circuit has been found to be tightly linked to mood and anxiety disorders (Shin et al., 2004). Anatomically, IL and amygdala share dense reciprocal connections (McDonald, 1998; Russchen, 1982a, 1982b; Sesack et al., 1989). These physical connections provide the anatomical basis of the observed anticorrelated RSFC between the two regions. More importantly, there is substantial evidence suggesting IL could exert inhibitory regulation on amygdala. For instance, electrical stimulation of IL reduces responsiveness of central nucleus output neurons in the amygdala to basolateral amygdala (BLA) stimulation (Quirk et al., 2003), and

chemical stimulation of IL activate cFos in the ITC neurons which are known to inhibit central nucleus output neurons (Pare and Smith, 1993). These results collectively suggest that the anticorrelated relationship between amygdala and IL observed in the present study could arise from an inhibitory interaction between them.

Time-frequency dynamics

One recent human study examined the anticorrelation between DMN and TPN by employing WTC and found that the anticorrelation between these two networks was not static (Chang and Glover, 2010). In the present study, wavelet analysis revealed a more stable anti-phase relationship between spontaneous BOLD fluctuations from IL and amygdala in awake rats. This difference may suggest a stronger anticorrelated relationship over time in rats and may also explain why it can be observed even in the mask of the global signal.

The influence of motion

In the present study, effects of movement in rats was minimized by using (i) motion correction; (ii) discarding data sets with excessive movement (> 0.5 mm, 17 sessions in total); and (iii) regressing out motion correction covariates. However, we did notice that movement of awake rats was significantly larger than that of anesthetized rats. There is the possibility that the difference in anticorrelation between awake and anesthetized rats was due to different levels of movement during data acquisition. To rule out this possibility, data from awake rats with minimal movement (< 0.125 mm, i.e. ¼ voxel size) were selected (33 sessions in total, 27.3% of the whole data set). In this subgroup, movement in awake rats was not significantly different from anesthetized rats (two-sample t-test, $p = 0.19$). Figure 8 showed that strong anticorrelated RSFC between amygdala and IL was persistent in this subgroup. This result suggests that the anticorrelated RSFC observed in the present study cannot be attributed to the factor of movement.

Limitations and Future implications

Although the current study has shown for the first time robust fMRI anticorrelation in a system with known inhibitory connections, it cannot resolve the debate on the origin of anticorrelations in humans. There are important differences between the rat and human results which prohibit this extension. First, the rat anticorrelations are present even prior to global regression, but the human anticorrelations are not. Second, the rat anticorrelations are between two specific anatomic regions with known strong anatomical connections, the human anticorrelations are between two wide-spread networks. Nevertheless, the finding of this study makes it possible to uncover the neurophysiologic basis of anticorrelated RSFC when combining with other techniques such as neuron recordings. Since anticorrelated RSFC represents a group of functional connections with distinct neurophysiologic features, it can tremendously contribute to studies of neural circuitriess and brain networks. More importantly, given the vital role that RSFC plays in regulating brain function at normal and pathological conditions, the results of the present study can help test the hypothesis that negative RSFC might serve as an important biomarker to evaluate the functionality of neural circuits at normal and pathological conditions. Therefore, the present study has opened a new avenue to further expanding the applicability of rsfMRI.

Acknowledgments

We thank Dr Wei Huang and Ms Meghan Heffernan for their technical assistance. We also would like to thank anonymous reviewers for their insightful comments. This publication was made possible by the NIH Grant Number 1R01 MH067096-02 (PI: Jean King, PhD) and 5R01DA021846-02 (PI: Jean King, PhD) from the National Institute of Health, and the institutional fund from the University of Massachusetts Medical School. Its contents are solely the responsibility of the authors and do not necessarily represent the official views of the NIH.

References

Albert NB, Robertson EM, Miall RC. The resting human brain and motor learning. Curr Biol. 2009; 19:1023–1027. [PubMed: 19427210]

Amano T, Unal CT, Pare D. Synaptic correlates of fear extinction in the amygdala. Nat Neurosci. 2010; 13:489–494. [PubMed: 20208529]

Anderson JS, Druzgal TJ, Lopez-Larson M, Jeong EK, Desai K, Yurgelun-Todd D. Network anticorrelations, global regression, and phase-shifted soft tissue correction. Hum Brain Mapp. 32:919–934. [PubMed: 20533557]

Berretta S, Pantazopoulos H, Caldera M, Pantazopoulos P, Pare D. Infralimbic cortex activation increases c-Fos expression in intercalated neurons of the amygdala. Neuroscience. 2005; 132:943–953. [PubMed: 15857700]

Biswal B, Yetkin FZ, Haughton VM, Hyde JS. Functional connectivity in the motor cortex of resting human brain using echo-planar MRI. Magn Reson Med. 1995; 34:537–541. [PubMed: 8524021]

Chang C, Glover GH. Effects of model-based physiological noise correction on default mode network anti-correlations and correlations. Neuroimage. 2009; 47:1448–1459. [PubMed: 19446646]

Chang C, Glover GH. Time-frequency dynamics of resting-state brain connectivity measured with fMRI. Neuroimage. 2010; 50:81–98. [PubMed: 20006716]

Forman SD, Cohen JD, Fitzgerald M, Eddy WF, Mintun MA, Noll DC. Improved assessment of significant activation in functional magnetic resonance imaging (fMRI): use of a cluster-size threshold. Magn Reson Med. 1995; 33:636–647. [PubMed: 7596267]

Fox MD, Snyder AZ, Vincent JL, Corbetta M, Van Essen DC, Raichle ME. The human brain is intrinsically organized into dynamic, anticorrelated functional networks. Proc Natl Acad Sci U S A. 2005; 102:9673–9678. [PubMed: 15976020]

Fox MD, Zhang D, Snyder AZ, Raichle ME. The global signal and observed anticorrelated resting state brain networks. J Neurophysiol. 2009; 101:3270–3283. [PubMed: 19339462]

Greicius MD, Flores BH, Menon V, Glover GH, Solvason HB, Kenna H, Reiss AL, Schatzberg AF. Resting-state functional connectivity in major depression: abnormally increased contributions from subgenual cingulate cortex and thalamus. Biol Psychiatry. 2007; 62:429–437. [PubMed: 17210143]

Greicius MD, Krasnow B, Reiss AL, Menon V. Functional connectivity in the resting brain: a network analysis of the default mode hypothesis. Proc Natl Acad Sci U S A. 2003; 100:253–258. [PubMed: 12506194]

Grinsted A, Moore JC, Jevrejeva S. Application of the cross wavelet transform and wavelet coherence to geophysical time series. Nonlinear Processes in Geophysics. 2004; 11:561–566.

Hampson M, Driesen N, Roth JK, Gore JC, Constable RT. Functional connectivity between task-positive and task-negative brain areas and its relation to working memory performance. Magn Reson Imaging. 2010; 28:1051–1057. [PubMed: 20409665]

Hampson M, Peterson BS, Skudlarski P, Gatenby JC, Gore JC. Detection of functional connectivity using temporal correlations in MR images. Hum Brain Mapp. 2002; 15:247–262. [PubMed: 11835612]

Horovitz SG, Braun AR, Carr WS, Picchioni D, Balkin TJ, Fukunaga M, Duyn JH. Decoupling of the brain's default mode network during deep sleep. Proc Natl Acad Sci U S A. 2009; 106:11376–11381. [PubMed: 19549821]

Kelly AM, Uddin LQ, Biswal BB, Castellanos FX, Milham MP. Competition between functional brain networks mediates behavioral variability. Neuroimage. 2008; 39:527–537. [PubMed: 17919929]

Kennedy DP, Redcay E, Courchesne E. Failing to deactivate: resting functional abnormalities in autism. Proc Natl Acad Sci U S A. 2006; 103:8275–8280. [PubMed: 16702548]

King JA, Garelick TS, Brevard ME, Chen W, Messenger TL, Duong TQ, Ferris CF. Procedure for minimizing stress for fMRI studies in conscious rats. J Neurosci Methods. 2005; 148:154–160. [PubMed: 15964078]

LeDoux JE. Emotion circuits in the brain. Annu Rev Neurosci. 2000; 23:155–184. [PubMed: 10845062]

Liang Z, King J, Zhang N. Uncovering intrinsic connectional architecture of functional networks in awake rat brain. J Neurosci. 2011; 31:3776–3783. [PubMed: 21389232]

Likhtik E, Pelletier JG, Paz R, Pare D. Prefrontal control of the amygdala. J Neurosci. 2005; 25:7429–7437. [PubMed: 16093394]

Liu X, Zhu XH, Zhang Y, Chen W. Neural Origin of Spontaneous Hemodynamic Fluctuations in Rats under Burst-Suppression Anesthesia Condition. Cereb Cortex. 2010; 21:374–384. [PubMed: 20530220]

Lowe MJ, Mock BJ, Sorenson JA. Functional connectivity in single and multislice echoplanar imaging using resting-state fluctuations. Neuroimage. 1998; 7:119–132. [PubMed: 9558644]

Lu H, Zuo Y, Gu H, Waltz JA, Zhan W, Scholl CA, Rea W, Yang Y, Stein EA. Synchronized delta oscillations correlate with the resting-state functional MRI signal. Proc Natl Acad Sci U S A. 2007; 104:18265–18269. [PubMed: 17991778]

McDonald AJ. Cortical pathways to the mammalian amygdala. Prog Neurobiol. 1998; 55:257–332. [PubMed: 9643556]

Murphy K, Birn RM, Handwerker DA, Jones TB, Bandettini PA. The impact of global signal regression on resting state correlations: are anti-correlated networks introduced? Neuroimage. 2009; 44:893–905. [PubMed: 18976716]

Pape HC, Pare D. Plastic synaptic networks of the amygdala for the acquisition, expression, and extinction of conditioned fear. Physiol Rev. 2010; 90:419–463. [PubMed: 20393190]

Pare D, Smith Y. The intercalated cell masses project to the central and medial nuclei of the amygdala in cats. Neuroscience. 1993; 57:1077–1090. [PubMed: 8309544]

Peltier SJ, Kerssens C, Hamann SB, Sebel PS, Byas-Smith M, Hu X. Functional connectivity changes with concentration of sevoflurane anesthesia. Neuroreport. 2005; 16:285–288. [PubMed: 15706237]

Phelps EA, Delgado MR, Nearing KI, LeDoux JE. Extinction learning in humans: role of the amygdala and vmPFC. Neuron. 2004; 43:897–905. [PubMed: 15363399]

Phelps EA, LeDoux JE. Contributions of the amygdala to emotion processing: from animal models to human behavior. Neuron. 2005; 48:175–187. [PubMed: 16242399]

Quirk GJ, Gehlert DR. Inhibition of the amygdala: key to pathological states? Ann N Y Acad Sci. 2003; 985:263–272. [PubMed: 12724164]

Quirk GJ, Likhtik E, Pelletier JG, Pare D. Stimulation of medial prefrontal cortex decreases the responsiveness of central amygdala output neurons. J Neurosci. 2003; 23:8800–8807. [PubMed: 14507980]

Rosenkranz JA, Grace AA. Dopamine attenuates prefrontal cortical suppression of sensory inputs to the basolateral amygdala of rats. J Neurosci. 2001; 21:4090–4103. [PubMed: 11356897]

Russchen FT. Amygdalopetal projections in the cat. I. Cortical afferent connections. A study with retrograde and anterograde tracing techniques. J Comp Neurol. 1982a; 206:159–179. [PubMed: 7085926]

Russchen FT. Amygdalopetal projections in the cat. II. Subcortical afferent connections. A study with retrograde tracing techniques. J Comp Neurol. 1982b; 207:157–176. [PubMed: 7096644]

Scholvinck ML, Maier A, Ye FQ, Duyn JH, Leopold DA. Neural basis of global resting-state fMRI activity. Proc Natl Acad Sci U S A. 2010; 107:10238–10243. [PubMed: 20439733]

Sesack SR, Deutch AY, Roth RH, Bunney BS. Topographical organization of the efferent projections of the medial prefrontal cortex in the rat: an anterograde tract-tracing study with Phaseolus vulgaris leucoagglutinin. J Comp Neurol. 1989; 290:213–242. [PubMed: 2592611]

Shin LM, Orr SP, Carson MA, Rauch SL, Macklin ML, Lasko NB, Peters PM, Metzger LJ, Dougherty DD, Cannistraro PA, Alpert NM, Fischman AJ, Pitman RK. Regional cerebral blood flow in the amygdala and medial prefrontal cortex during traumatic imagery in male and female Vietnam veterans with PTSD. Arch Gen Psychiatry. 2004; 61:168–176. [PubMed: 14757593]

Stevens WD, Hasher L, Chiew KS, Grady CL. A neural mechanism underlying memory failure in older adults. J Neurosci. 2008; 28:12820–12824. [PubMed: 19036975]

Vincent JL, Patel GH, Fox MD, Snyder AZ, Baker JT, Van Essen DC, Zempel JM, Snyder LH, Corbetta M, Raichle ME. Intrinsic functional architecture in the anaesthetized monkey brain. Nature. 2007; 447:83–86. [PubMed: 17476267]

Zhang N, Rane P, Huang W, Liang Z, Kennedy D, Frazier JA, King J. Mapping resting-state brain networks in conscious animals. J Neurosci Methods. 2010; 189:186–196. [PubMed: 20382183]

Research Highlights

- Functional connectivity in a frontolimbic circuit was measured in awake rats.
- Anticorrelation independent of preprocessing methods within this circuit was found.
- The anticorrelation contained high anatomical specificity and was reproducible.
- This anticorrelated relationship was absent in anesthetized rats.

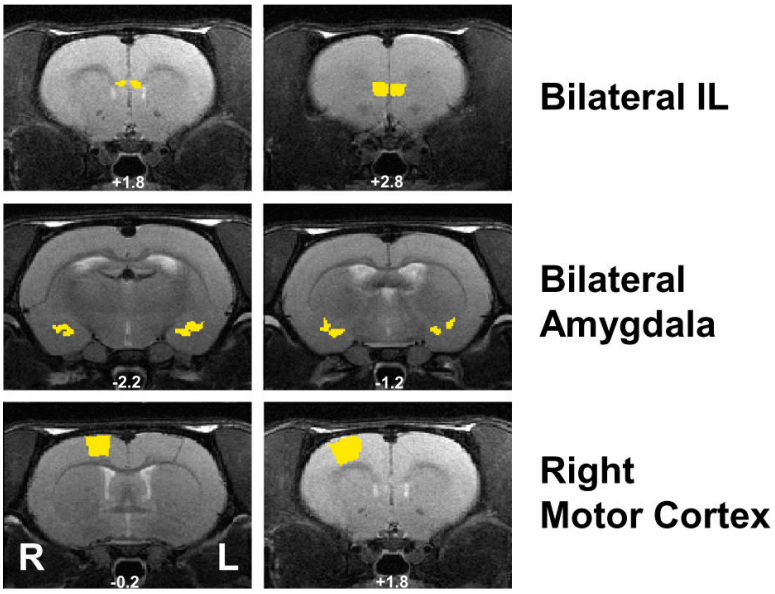

Figure 1.
Seed ROI definitions. Three seed ROIs were used in the present study: bilateral infralimbic cortex (IL), bilateral amygdala and unilateral (right) motor cortex. All ROIs were defined based on a fully segmented standard rat atlas in MIVA and overlaid on anatomical images (Liang et al., 2011; Zhang et al., 2010). Distances to Bregma (mm) are labeled at the bottom of each image.

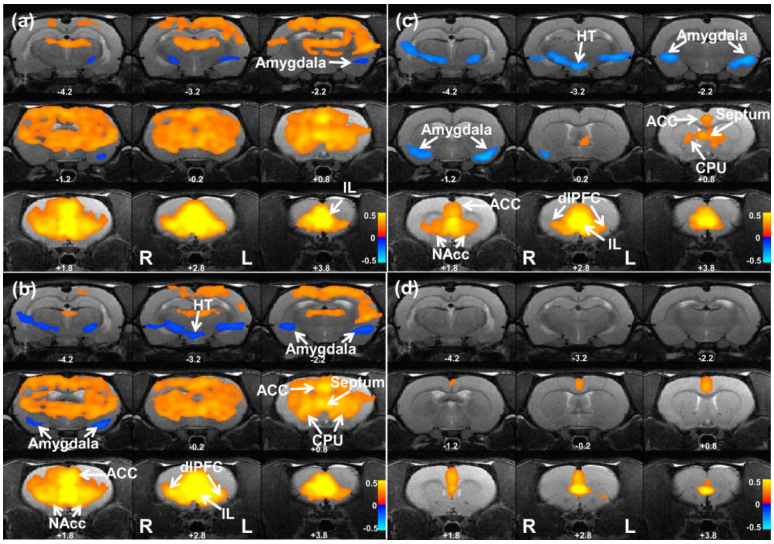

Figure 2.

IL RSFC maps. (a) The IL RSFC map in the awake condition without correction of any global signal. (b) The IL RSFC map in the awake condition with correction of the ventricle and white matter signal. (c) The IL RSFC map in the awake condition with correction of the global signal. (d) The IL RSFC map in the anesthetized condition with correction of the global signal. Data from all maps were corrected for six movement parameters. All maps were overlaid on anatomical images. Distances to Bregma (mm) are labeled at the bottom of each image.

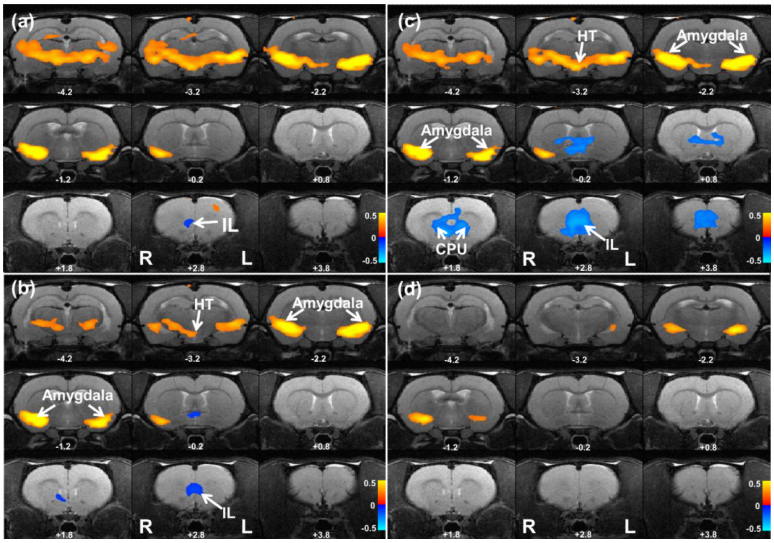

Figure 3.

Amygdala RSFC maps. (a) The Amygdala RSFC map in the awake condition without correction of any global signal. (b) The Amygdala RSFC map in the awake condition with correction of the ventricle and white matter signal. (c) The Amygdala RSFC map in the awake condition with correction of the global signal. (d) The Amygdala RSFC map in the anesthetized condition with correction of the global signal. Data from all maps were corrected for six movement parameters. All maps were overlaid on anatomical images. Distances to Bregma (mm) are labeled at the bottom of each image.

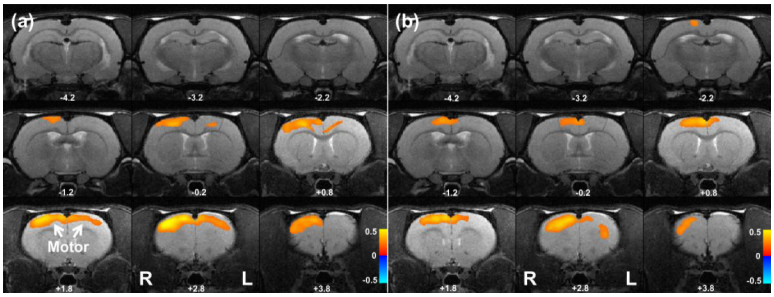

Figure 4.
RSFC maps from unilateral (right) motor cortex in (a) the awake condition and (b) the anesthetized condition. Both maps were obtained after global signal regression. Distances to Bregma (mm) are labeled at the bottom of each image.

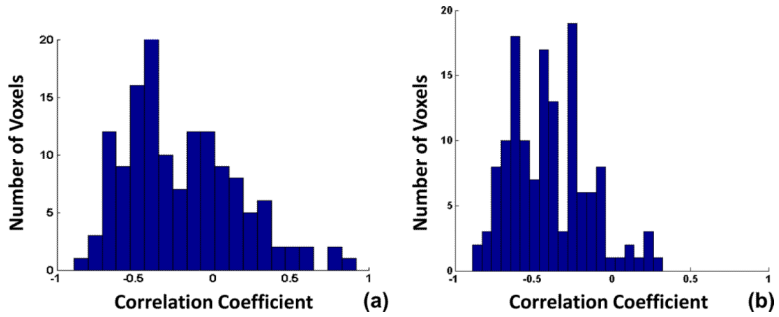

Figure 5.
Histograms of correlation coefficients between regional mean time courses of IL and amygdala (a) without and (b) with global signal regression.

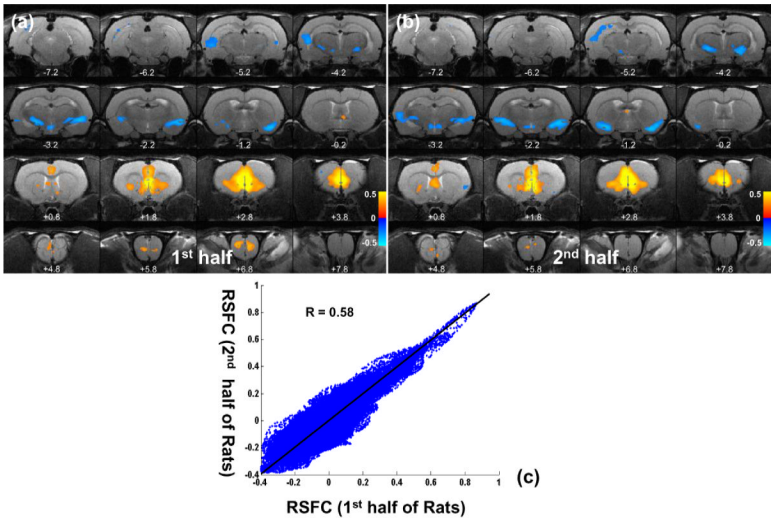

Figure 6.

Reproducibility of anticorrelation between IL and amygdala. Data from all animals were randomly divided into two subgroups. (a) The IL RSFC map generated from one subgroup with global signal regression. (b) The IL RSFC map generated from the other subgroup with global signal regression. Distances to Bregma (mm) are labeled at the bottom of each image. (c) The voxel-to-voxel correlation of the RSFC strength between the two subgroups.

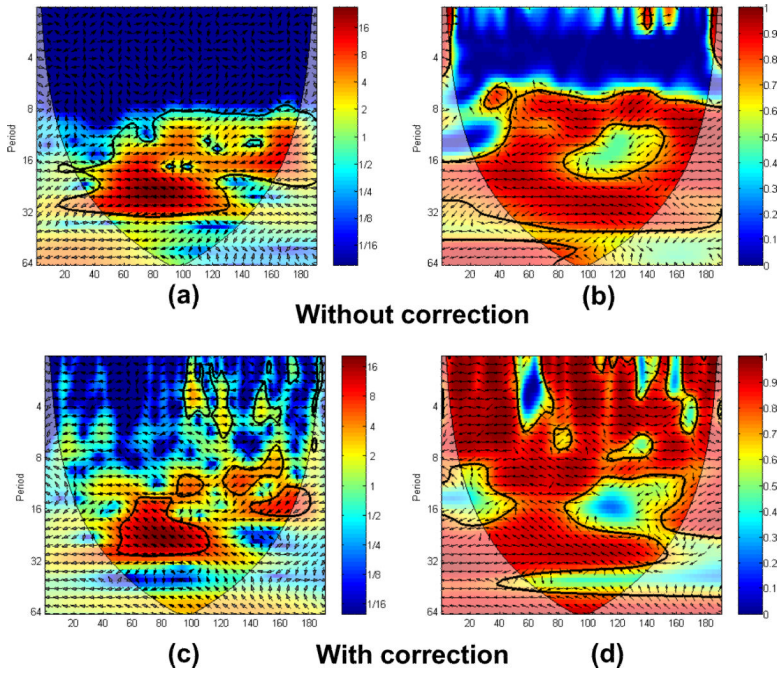

Figure 7.

Wavelet transform coherence analysis revealed anti-phase relationship between IL and amygdala. (a) Cross wavelet power of IL and amygdala time series from one representative RSFC run. (b) Cross wavelet coherence of IL and amygdala time series from the same RSFC run. Time series in (a) and (b) were not corrected for the global signal. (c) Cross wavelet power of IL and amygdala time series from the same RSFC run after global signal regression. (d) Cross wavelet coherence of IL and amygdala time series after global signal regression. X axis represents time (sec) and Y axis represents period.

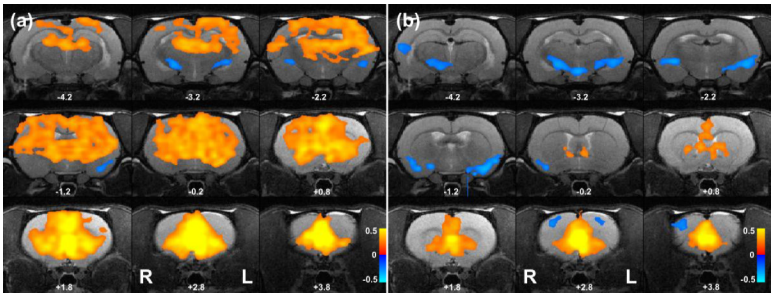

Figure 8.

IL RSFC maps from a subgroup of awake rats with movement smaller than 0.125mm (a) without and (b) with global signal regression. Movement in this subgroup was similar to that in anesthetized rats (two sample t-test, $p = 0.19$).